Ceramics International **23** (1997) 171–177

PII: S0272-8842(96)00019-3
0272-8842/97 $17.00+.00

Influences of Powder Preparation Routes on the Sintering Behaviour of Doped ZrO_2–3 mol%Y_2O_3

Y. H. Chiou & S. T. Lin

Mechanical Engineering Department, National Taiwan Institute of Technology, Taipei, Taiwan

(Received 19 April 1995; accepted 28 November 1995)

Abstract: The structural evolution and properties of ZrO_2–3 mol%Y_2O_3 doped with 2 mol%Al_2O_3–1 mol%MnO–1 mol%CoO–1 mol%SiO_2 were investigated. Three powder preparation routes with different degrees of distribution uniformity of the dopants in the zirconia powder were compared. With increasing distribution uniformity of the dopants in the zirconia powder, the relative dimension of the as-polished defects (pores and pull-out voids) decreased, while the concentration of the monoclinic phase increased as a result of enhanced dissolution of yttria into the intergranular glass phase. Optimized properties had been achieved when the powder having an intermediate degree of distribution uniformity of the dopants in the zirconia powder was utilized by precipitating the ions of the dopants on to the zirconia powder surface. © 1997 Elsevier Science Limited and Techna S.r.l.

1 INTRODUCTION

Tetragonal zirconia polycrystal (TZP) is a popular engineering ceramic material because of its excellent mechanical properties, especially a high fracture toughness value. The high fracture toughness is associated with the retention of a tetragonal phase, which transforms into monoclinic phase under applied stress by various mechanisms.[1] Stabilizers such as MgO, CaO, Y_2O_3, CeO_2 are used to retain the tetragonal phase after sintering, among which yttria is the most commonly used. The retention of tetragonal phase after sintering is possible if the grain size of the dense polycrystalline materials is smaller than a critical size, which depends on the yttria content.[1] However, the omnipresence of the liquid phase arising from powder impurities or additives causes the repartition of yttria during sintering. Repartition of yttria to the boundaries of zirconia grains, which is faster in an impurity richer powder, causes enhanced grain growth when the phase repartition has finished.[2]

Doping of transitional metal oxides has been applied to change the properties of oxide ceramics. Examples include modifying pore structure,[3] altering colour,[4] and improving high temperature superplastic behaviour.[5,6] The success of these examples depends strongly on the distribution uniformity of the dopants in the zirconia matrix, and, thereby, the influences of the dopants on the microstructural evolution at elevated temperatures. The incentives of this study were to alter the colour, control the defect structure after polishing, and retain the mechanical properties of TZP by doping a small quantity of mixed oxides. Different powder preparation routes were compared with respect to the undoped powder. The powder preparation routes, in the order of increasing distribution uniformity of the dopants in the zirconia powder, including ball-milling of the dopants with the zirconia powder, precipitation of the ions of the dopants on to the zirconia powder surface from a water solution, and co-precipitation of the ions of the dopants and zirconia from a water solution. The design concepts of these powder preparation routes are analogous to the mixed powder, coated composite powder, and pre-alloyed powder used in metal powders, which represent different degrees of alloying uniformity and, subsequently, different sintering performances.

2 EXPERIMENTAL PROCEDURES

The composition of the doped zirconia was (ZrO_2–3 mol%Y_2O_3)–2 mol%Al_2O_3–1 mol%MnO–1 mol%CoO–1 mol%SiO_2. Three different powder preparation routes, designated as ball-milling, coating, and co-precipitation, were compared along with the undoped ZrO_2–3 mol%Y_2O_3. These powder preparation routes are described in the following.

2.1 Ball-milling

A commercial grade ZrO_2–3 mol%Y_2O_3 (HYS 3.0, Daiichi Kigenso Kagaku Kogaku Co., Ltd, Japan) was wet-milled with Al_2O_3 powder (average particle size: 0.5 μm), MnO powder (average particle size: 2.5 μm), CoO powder (average particle size: 0.82 μm), and SiO_2 powder (average particle size: 4.3 μm) for 10 h. The milling medium was a solution of 10 vol% paraffin wax (based on powder volume) dissolved in

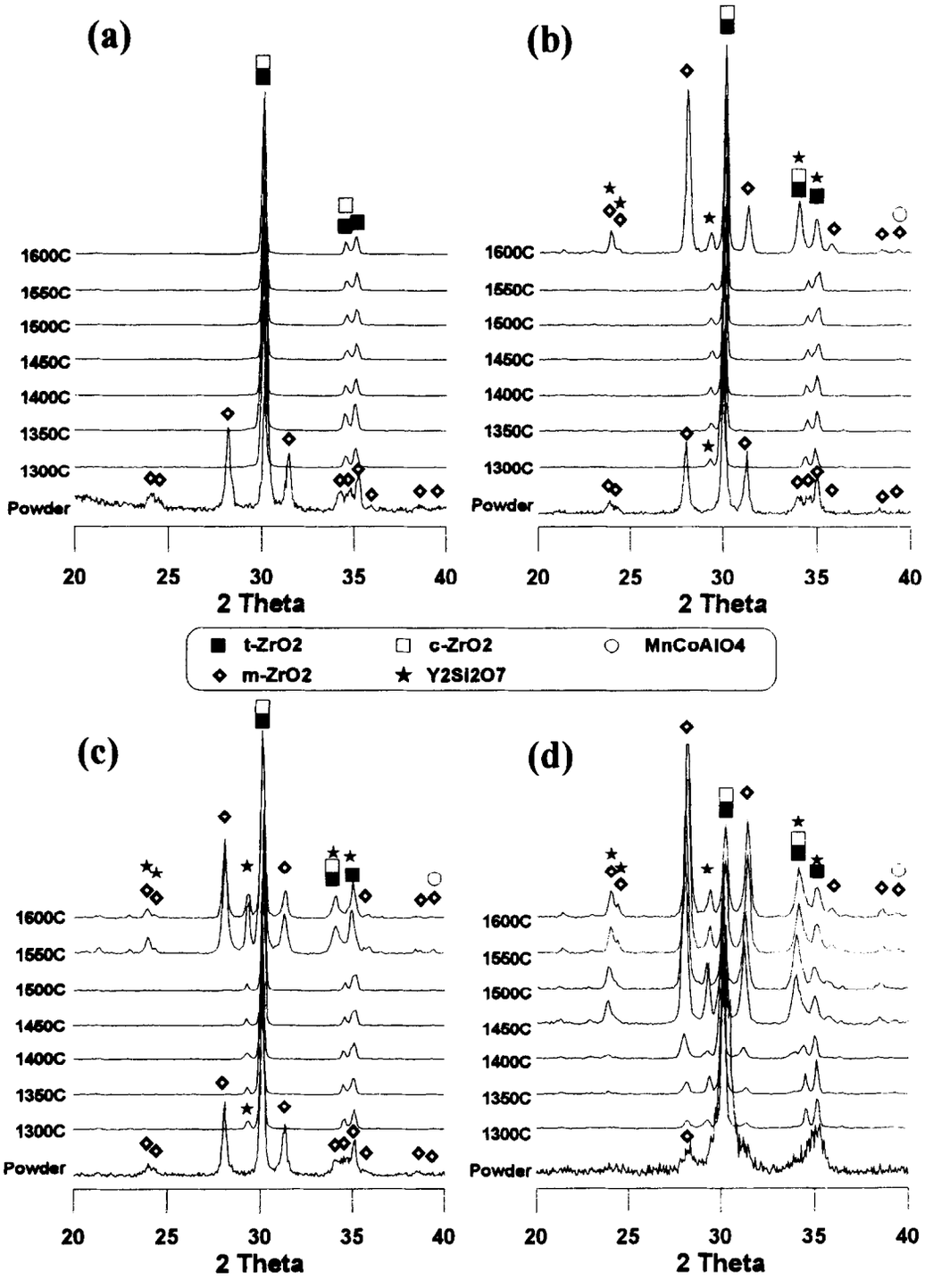

Fig. 1. X-ray diffraction patterns of undoped and doped ZrO_2–3 mol%Y_2O_3 powders in the powder state and sintered state. (a) Undoped powder, and doped powders by (b) ball-milling, (c) coating, and (d) co-precipitation.

heptane and the milling balls were high purity tetragonal zirconia polycrystalline balls.

2.2 Coating

The commercial grade ZrO_2–3 mol%Y_2O_3 powder used in ball-milling was also used in this preparation route. The precursors for the oxide additives were $AlCl_3 \cdot 6H_2O$, $MnCl_2 \cdot 6H_2O$, $CoCl_2 \cdot 6H_2O$ and $SiCl_4$. The zirconia powder was initially maintained in an ammonia water solution (pH = 12), and constantly stirred with an ultrasonic oscillator. The metal chlorides as the oxide precursors were initially dissolved in deionized water and then slowly dripped into the ammonia water solution that contained the zirconia powder. The metal ions thus precipitated on to the zirconia powder surface in the form of hydrated metal hydroxides. The coated zirconia powder was washed twice with deionized water to remove the residual unprecipitated ions. The powder was subsequently calcined at 800 °C for 1 h and ball-milled according to the same procedures as were used for the ball-milled powder except that the milling time was 4 h.

2.3 Co-precipitation

Metal oxide precursors, including $ZrOCl_2 \cdot 8H_2O$, $Y(NO_3)_3 \cdot 5H_2O$, and those chlorides used in the coating route, were first dissolved in deionized water. The solution was then slowly dripped into an ammonia water solution (pH = 12), which was constantly stirred with an ultrasonic oscillator. The precipitated powder in the form of hydrated metal hydroxides was washed twice with deionized water and calcined at 800 °C for 1 h. The same ball-milling procedures as those of the coating route were applied to disperse the agglomerated powder.

The powders were uniaxially pressed at a pressure of 30 MPa into disks having the dimensions of 16 mm in diameter and 5 mm in height. The specimens were sintered in air. The thermal profile was a ramp of 3 K/min. to 500 °C, held for 30 min., and followed by a ramp of 10 K/min. to the sintering temperature (1300–1600 °C), held for 1 h.

X-ray diffraction patterns of the powders and the as-sintered specimens were recorded using nickel filtered Cu Kα radiation (XRD, Rigaku D Max B). The relative abundance of the monoclinic phase was calculated based on the equation developed by Howard,[7] and the lattice constant ratio (c/a) was calculated from the lattice constants generated from the attached software.[8] The sintered density was measured by water immersion method. The specimens were then relief-polished using an automatic machine. The hardness and fracture toughness were determined using a Vickers microhardness indentor under the loads of 9.8 N and 245 N, respectively.[9] Optical microscope was used to examine the pore structure of the polished surface. Scanning electron microscope (SEM) was used to reveal the morphology of the thermally etched surface (1300 °C for 2 h). Additionally, phase identification of a sintered specimen was carried out using scanning transmission electron microscope (STEM) attached with energy dispersive X-ray analysis (EDXA).

3 RESULTS AND DISCUSSION

Figure 1 shows the XRD patterns of the powder and sintered compacts for the undoped and doped powders. The as-received ZrO_2–$3Y_2O_3$ powder showed strong characteristic diffraction peaks of the monoclinic phase, indicating that the co-precipitation of Y_2O_3 and ZrO_2 was not uniform during the azeotropic distillation.[10,11] For a sintering temperature higher than 1300 °C, the monoclinic phase of the zirconia virtually disappeared as a result of the dissolution of Y_2O_3 into the ZrO_2 grains. Similar structural development patterns were observed for the doped powders, except the reappearance of the monoclinic phase of zirconia at various sintering temperatures and the crystallization of a yttria and silica based compound

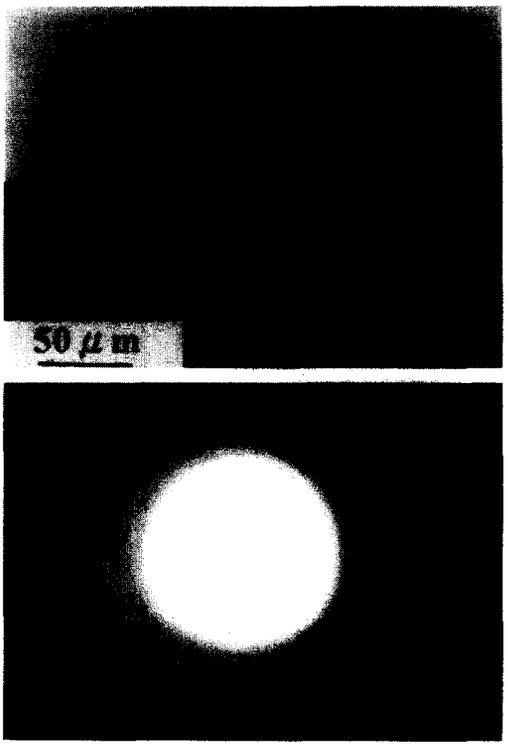

Fig. 2. STEM micrograph and selected area electron diffraction pattern of a glass phase exuded out of the zirconia grains for the coated powder sintered at 1300 °C (camera length, 100 cm; accelerating voltage, 160 kV).

($Y_2Si_2O_7$). The relative concentrations of the monoclinic phase of zirconia and $Y_2Si_2O_7$ increased with increased sintering temperature, indicating the repartitioning of yttria from the zirconia grains toward the intergranular glass phase was preferred. Figure 2 shows the STEM micrograph of a silica-rich glass phase that had exuded out of the zirconia grains, for a specimen prepared with the coated powder and sintered at 1300 °C.

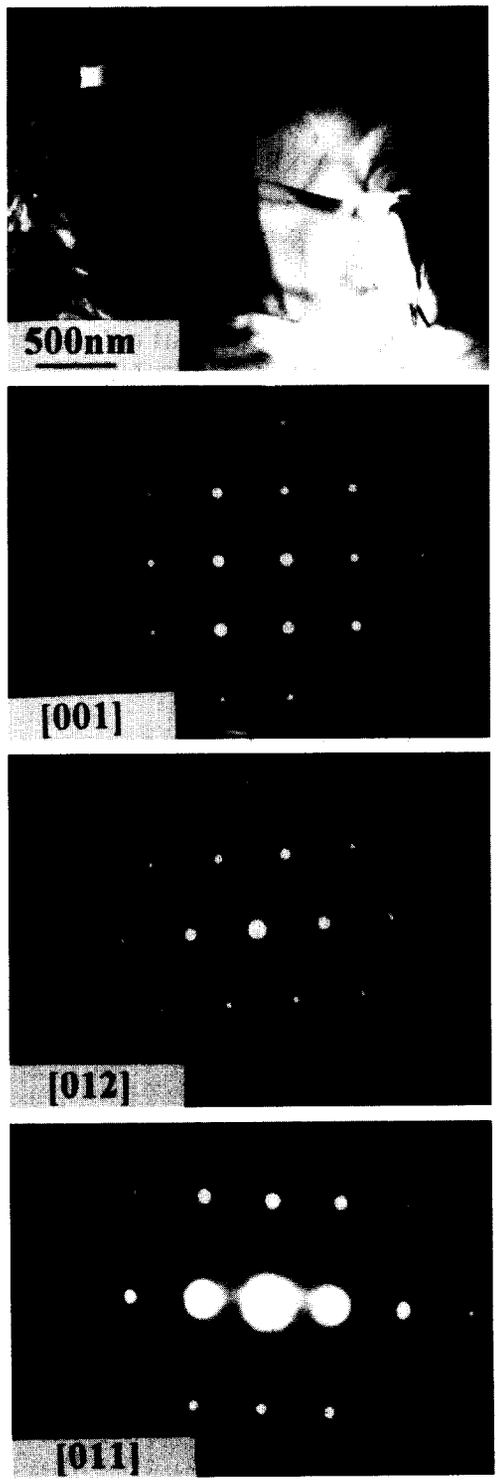

Fig. 3. STEM micrograph and selected area electron diffraction patterns of a $MnCoAlO_4$ spinel phase for the coated powder sintered at 1300 °C (camera length, 100 cm; accelerating voltage, 160 kV).

The glass phase was principally composed of Si, Y and Zr, based on EDXA analysis. Out of the amorphous phase there precipitated a lot of fine particles. These fine particles were possibly the yttria and silica based compound, $Y_2Si_2O_7$, found in the XRD patterns. The lack of a high concentration of Al, Co and Mn ions in the glass phase indicated that these ions could have possibly segregated together during sintering, similar to that observed for a tetragonal zirconia polycrystal doped with Al_2O_3 and CoO.[4] Figure 3 shows a STEM micrograph and the selected area diffraction patterns for a specimen prepared with the coated powder and sintered at 1300 °C. A $MnCoAlO_4$ spinel phase was identified based on EDXA composition analysis of the selected area electron diffraction patterns. In such a manner, the highly evaporative colourants, CoO and MnO, were secured by reacting with Al_2O_3 at low temperatures.

Figure 4 shows the variation of the lattice constant ratio (c/a) and the relative abundance of the monoclinic phase of zirconia with sintering temperature for the four powders. The relative abundance of the monoclinic phase of zirconia was strongly correlated with the (c/a) ratio. The undoped powder, whose c/a ratio was very consistent in the temperature range investigated, showed a very low concentration of the monoclinic

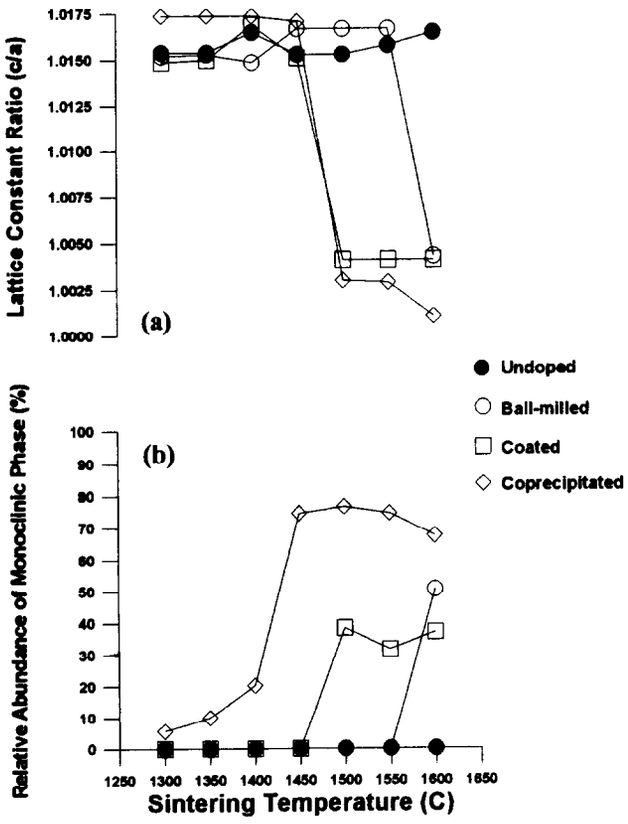

Fig. 4. Variation of the lattice constant ratio (c/a) and the relative abundance of the monoclinic phase of zirconia with sintering temperature for the undoped and doped powders.

phase of zirconia. In contrast, the increased concentration of the monoclinic phase of zirconia for the doped powders was accompanied by the decrease of the c/a ratio. A decrease of the c/a ratio indicated the loss of the transformability of zirconia.[12]

The development of a substantial concentration of the monoclinic phase of zirconia for the ball-milled powder, coated powder and co-precipitated powder were 1600 °C, 1500 °C and 1450 °C, respectively. The formation of the monoclinic phase of zirconia was promoted by the enhanced distribution uniformity of the dopants in the zirconia powder. For metallic powders, the formation of a liquid phase at temperatures higher than the eutectic temperature was fast for a pre-alloyed powder compared with the mixed elemental powders having the equivalent composition. In a similar manner, the formation of the silica based glass phase was enhanced by a higher distribution uniformity of Si atoms in the zirconia powder. Therefore, evolution of the monoclinic phase of zirconia was promoted as yttria dissolved into the glass phase.

Figure 5 shows the as-polished surface of the doped powders sintered at 1300 °C. The relative dimension of the defects (pores and pull-out voids) decreased with the increase of the relative distribution uniformity of the dopants in the powder. Additionally, the shape of the large defects existing in the sintered compact prepared with the coated powder was similar to that of an arch. Based on these observations, the defects in the sintered compacts partially reflected the segregation states of the dopants in the green compacts. As a consequence, homogenization of the dopants was not fully achieved after sintering. Figure 6 shows the

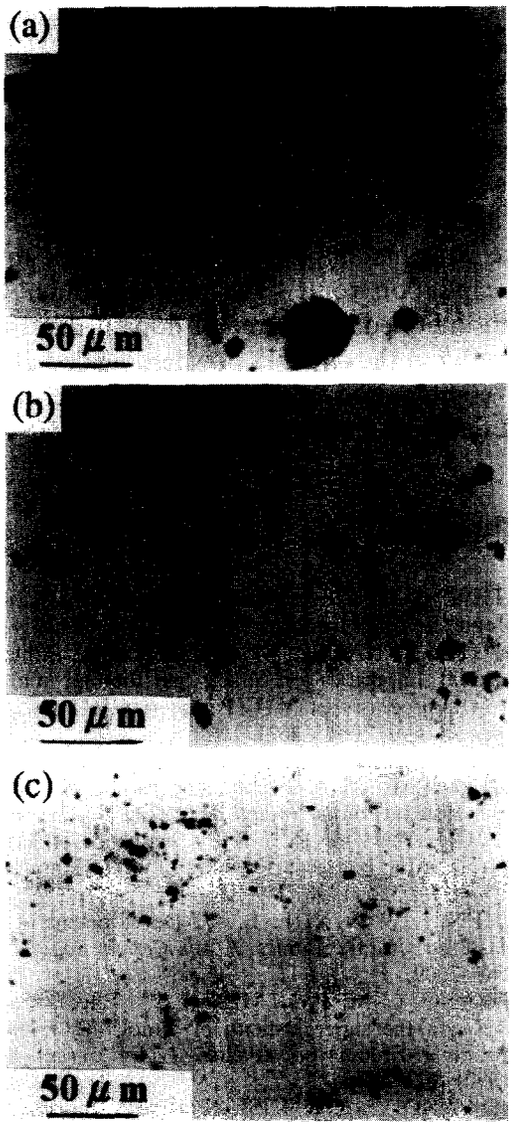

Fig. 5. As-polished surface of the doped powders sintered at 1300 °C, showing the significant difference in the size and shape of the defects (pores and pull-out voids) for powders prepared from (a) ball-milling, (b) coating, and (c) co-precipitation routes.

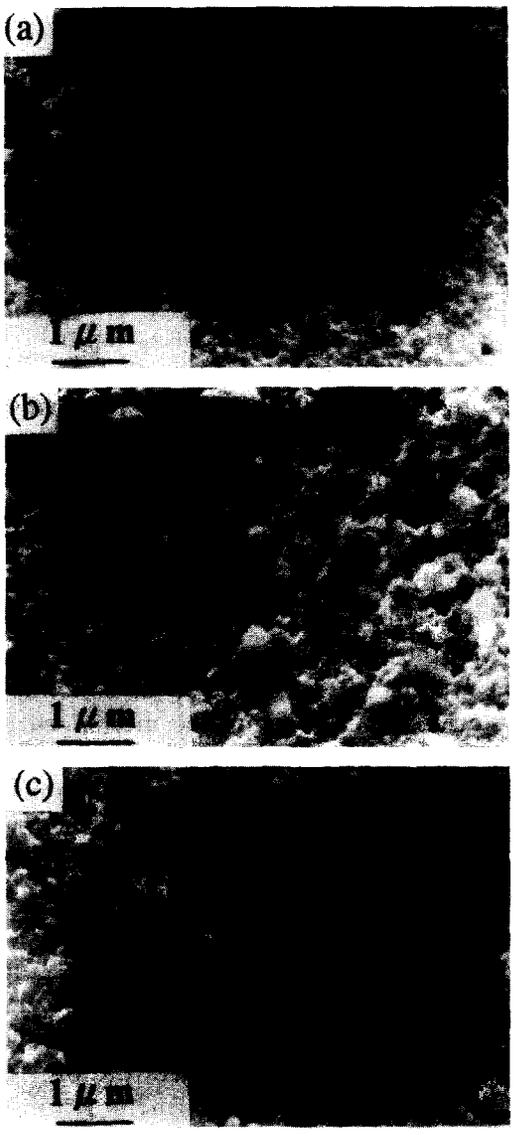

Fig. 6. Etch microstructures for the doped powders sintered at 1300 °C, showing the segregation states of the $MnCoAlO_4$ spinel phase for the powders prepared from (a) ball-milling, (b) coating, and (c) co-precipitation routes.

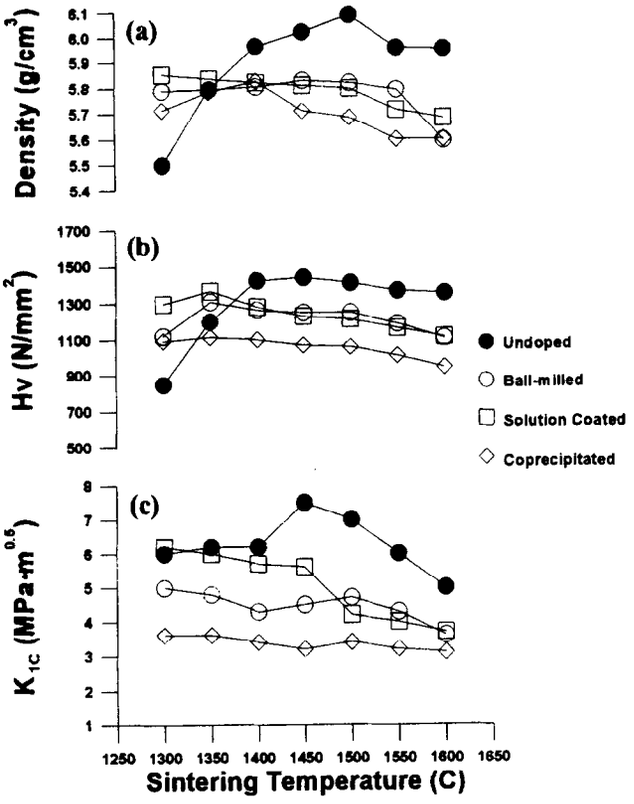

Fig. 7. Variation of density, microhardness and fracture toughness with sintering temperature for the undoped and doped powders.

etched microstructures for the doped zirconia sintered at 1300 °C. As was expected, the relative dimension of the $MnCoAlO_4$ spinel phase decreased with the increase of the distribution uniformity of the dopants in the zirconia powder. The grains of the spinel phase aggregated very severely for sintered compact prepared with the ball-milled powder. However, the grains of the spinel phase could hardly be differentiated from the zirconia grains for the sintered compact prepared with the co-precipitated powder.

One of the most critical criteria for preparing coloured TZPs is the reduction of sintering temperature without sacrificing the mechanical properties. A low sintering temperature can reduce the loss of the colour additives because of their high vapour pressure,[13] and increase the growth of the zirconia grains arising from the existence of liquid channels with a high diffusivity.[14] Figure 7 shows the variation of density, microhardness and fracture toughness with sintering temperature for the undoped and doped powders. The undoped powder exhibited a continuous increase of sintered density up to a sintering temperature of 1500 °C, whereas the hardness and fracture toughness reached their maximum values at 1450 °C. In contrast, the doped powders displayed optimum combinations of properties at temperatures between 1300 °C and 1350 °C. Among these doped powders, the coated powder showed hardness and fracture toughness comparable to those of the undoped powder at the sintering temperature of 1300 °C. Therefore, an intermediate degree of distribution uniformity of the dopants in the zirconia avoided the formation of large defects (pores and pull-out voids) arising from the dopant segregation, and loss of transformability of the zirconia phase arising from the intensive dissolution of yttria into the silica based glass phase.

4 CONCLUSION

Different powder preparation routes, including ball-milling, coating and co-precipitation, were shown to affect the microstructural evolution and mechanical properties of ZrO_2–3 mol%Y_2O_3 doped with 2 mol%Al_2O_3–1 mol%MnO–1 mol%CoO–1 mol%SiO_2. Severe macro-segregation of the dopants in the zirconia powder for the ball-milling route resulted in very large defects after polishing. The mechanical properties were severely degraded as dissolution of yttria from the zirconia grains into the silica based glass phase during sintering was promoted by the uniform distribution of the dopants in the zirconia powder for the co-precipitation route. The coating route, which had an intermediate degree of dopant distribution uniformity in the zirconia powder, yielded an optimum combination of mechanical properties and defect dimension after polishing.

REFERENCES

1. STEVENS, R., *Zirconia and Zirconia Ceramics*, 2nd edn. Magnesium Elektron Ltd, UK, 1986, pp. 17–26.
2. STOTO, T., NAUER, M. & CARRY, C., Influence of residual impurities on phase partitioning and grain growth processes of Y–TZP materials. *J. Am. Ceram. Soc.*, **74** (1991) 2615–2621.
3. KOSTIC, E., KISS, S. J. & BOSKOVIC, S., Sintering and microstructure development in the Al_2O_3–MnO–TiO_2 system. *Powder Metall. Int.*, **22** (1990) 29–30.
4. CHIOU, Y. H. & LIN, S. T., Influence of CoO and Al_2O_3 on the phase partitioning of ZrO_2–3 mol%Y_2O_3. *Ceram. Int.*, **22** (1996) 249–256.
5. CHEN, I. W. & XUE, L. A., Development of superplastic structural ceramics. *J. Am. Ceram. Soc.*, **73** (1990) 2585–2609.
6. HWANG, C. M. J. & CHEN, I. W., Effect of a liquid phase on the superplasticity of 2 mol%Y_2O_3-stabilized tetragonal zirconia polycrystals. *J. Am. Ceram. Soc.*, **73** (1990) 1626–1632.
7. HOWARD, C. J. & KISI, E. H., Polymorph method determination of monoclinic zirconia in partially stabilized zirconia ceramics. *J. Am. Ceram. Soc.*, **73** (1990) 3096–3099.
8. *JCPDS, Powder Diffraction File Search Manual: Hanawalt method, inorganic.* International Center for Diffraction Data, Swarthmore, PA, 1990.

9. EVANS, A. G. & CHARLES, E. A., Fracture toughness determinations by indentation. *J. Am. Ceram. Soc.*, **59** (1976) 371–372.
10. HAASE, I., YI, L., NICHT, E. M., XIAOXIAN, H. & JINKUN, G., Preparation and characterization of ultrafine zirconia powder. *Ceram. Int.*, **18** (1992) 343–351.
11. HIRANO, M. & INADA, H., Preparation, sintering, microstructure, and thermal stability of Y_2O_3- and CeO_2-doped tetragonal zirconia ceramics. *Ceram. Int.*, **17** (1991) 359–365.
12. KIM, D. J., Effects of Ta_2O_5, Nb_2O_5, and HfO_2 alloying on the transformability of Y_2O_3-stabilized tetragonal ZrO_2. *J. Am. Ceram. Soc.*, **73** (1990) 115–120.
13. NORTON, F. H., *Elements of Ceramics*, 2nd edn. Addison–Wesley, Reading, MA, 1974, pp. 126–127.
14. DILL, S., FRENCH, J. D., HARMER, M. P. & CHAN, H. M., Coarsening in duplex microstructures: The effect of liquid phase. *Bull. Am. Ceram. Soc.*, **71** (1992) 1554.